Available online at www.sciencedirect.com
ScienceDirect
Mendeleev Commun., 2014, **24**, 26–28
Mendeleev Communications

Characterization of a Pd^{II} complex with (*E*)-8-hydroxyquinoline-2-carbaldehyde *O*-benzyl oxime

Jan Grzegorz Małecki,*[a] Anna Maroń,[a] Izabela Gryca[a] and Maciej Serda[b]

[a] *Department of Crystallography, Institute of Chemistry, University of Silesia, 40-006 Katowice, Poland. E-mail: gmalecki@us.edu.pl*
[b] *Department of Organic Chemistry, Institute of Chemistry, University of Silesia, 40-006 Katowice, Poland*

DOI: 10.1016/j.mencom.2013.12.008

The title complex was synthesized and characterized by IR, NMR and UV-VIS spectroscopy and X-ray crystallography; the electronic structure of the complex was calculated using the density functional theory.

Palladium(II) complexes are of considerable current interest because of their potentially beneficial pharmacological properties. Palladium complexes with aromatic N-containing ligands, such as pyridine, quinoline, pyrazole and 1,10-phenanthroline derivatives, have shown very promising antitumor characteristics.[1–4] Some of these complexes, especially the *trans* analogues with nonplanar heterocyclic amine ligands, have been found to overcome multifactorial cisplatin resistance in human ovarian cell lines.[5,6] On the other hand, Pd^{II} complexes exhibited catalytic activity in carbon–carbon and carbon–nitrogen bond-forming reactions.[7,8] Four-coordinate palladium(II) complexes with square-planar geometry and various N-heteroaromatic ligands are useful building blocks for producing interesting molecular structures.[9] Metal complexes with N-heteroaromatic ligands exhibit luminescent properties, which strongly depend on their electronic structure.[10–14]

Here, we report the syntheses and spectroscopic characterization of (*E*)-8-hydroxyquinoline-2-carbaldehyde *O*-benzyl oxime (L) and a palladium(II) complex with the ligand L. The optically active 8-hydroxyquinoline derivatives are promising fluorogenic chelating agents in luminescence investigation, and may possess the capacity to contribute excellent emission when it works with coordinated metal ions. Moreover, we also performed a quantum-chemical study to characterize the molecular and electronic structures of the complex by the analysis of optimized molecular geometry and electronic populations using a natural bond orbitals scheme for identifying the nature of interactions between the ligands and the central ion. The time dependent density functional theory (TD-DFT) was finally used to calculate the electronic absorption spectrum. Based on a molecular orbital scheme, these results allowed us to interpret the absorption and emission spectra obtained at an experimental level.

(*E*)-8-Hydroxyquinoline-2-carbaldehyde *O*-benzyl oxime was prepared by microwave assisted synthesis,[†] and the palladium(II) complex was obtained by a reaction of the ligand with $PdCl_2$ (metal : ligand ratio, 1 : 2) in acetonitrile.[‡] The ligand and the complex were characterized by conventional spectroscopic techniques and single-crystal X-ray analysis.[§] The IR spectrum of the ligand shows a strong absorption band at 3422 cm^{-1} assignable to the O–H stretch, which is not present in the spectrum of the complex. Oxime C=N and C–O gave strong bands at 1640 and 1012 cm^{-1} in the ligand and 1647, 1027 cm^{-1} in the complex. The

[†] Synthesis was performed in a CEM discovery microwave reactor with temperature and pressure control. Equimolar quantities of 8-hydroxyquinoline-2-carbaldehyde and *O*-benzylhydroxylamine were dissolved in dry ethanol, and then two drops of AcOH were added as a catalyst. The resulting mixture was heated in a microwave reactor at 85 °C for 10 min (maximum microwave power, 50 W). After cooling, the precipitated yellow solid was filtered off, washed with diethyl ether and crystallized from MeOH. Yield, 83%. IR (KBr, ν/cm^{-1}): 3422 (s, ν_{OH}), 3028 (ν_{ArH}), 2942 (ν_{CH}), 1640 (C=N oxime), 1560 ($\nu_{CN/C=C}$), 1243 (δ_{OH}), 1012 (N–O oxime). ^{1}H NMR (DMSO-d_6, 400 MHz) δ: 9.85 (m, 1H, OH), 8.37 (s, 1H, CH), 8.32 (d, 1H, *J* 8.8 Hz), 7.90 (d, 1H, *J* 8.4 Hz), 7.49–7.39 (m, 7 H), 7.12 (d, 1H, *J* 8.8 Hz), 5.30 (s, 2 H, CH_2). ^{13}C NMR (DMSO-d_6, 100 MHz) δ: 153.94 (C–O_{quin}), 150.42 (CH–N–O), 149.66, 138.56, 137.69, 137.25, 129.24, 128.94, 128.90, 128.86, 128.49, 118.31, 118.24, 112.65, 76.63 (CH_2).

[‡] The mixture of (*E*)-8-hydroxyquinoline-2-carbaldehyde *O*-benzyl oxime (0.28 g, 1 mmol) and $PdCl_2$ (0.1 g, 0.5 mmol) in acetonitrile (50 cm^3) was refluxed for ~3 h. The yellow single crystals were obtained by slow evaporation of the solvent. Yield, 91% (0.33 g). IR (KBr, ν/cm^{-1}): 3027 (ν_{ArH}), 2926, 2873 (ν_{CH}), 1647 (C=N oxime), 1554 ($\nu_{CN/C=C}$), 1027 (N-O oxime). ^{1}H NMR (500 MHz, $CDCl_3$) δ: 8.37 (s), 8.01 (dd, *J* 10.7 and 8.7 Hz), 7.61 (*t*, *J* 11.9 Hz), 7.55–7.32 (m), 7.00 (d, *J* 7.9 Hz), 5.31 (s, CH_2). ^{13}C NMR (126 MHz, $CDCl_3$) δ: 167.95 (C–O_{quin}), 152.76 (CH–N–O), 149.79, 138.38, 136.36, 127.63, 119.47, 115.22, 113.01, 110.40, 76.78 (CH_2). UV-VIS [acetonitrile, λ/nm (log ε)]: 347 (3.16), 333 (3.41), 239 (sh), 212 (4.92).

[§] The X-ray intensity data of L and [$Pd(L)_2$] were collected on a Gemini A Ultra diffractometer equipped with an Atlas CCD detector and graphite monochromated MoKα radiation (α = 0.71073 Å) at room temperature. Lorentz, polarization and empirical absorption correction using spherical harmonics implemented in the SCALE3 ABSPACK scaling algorithm[19] were applied. The structure was solved by the Patterson method and subsequently completed by the difference Fourier recycling. All the non-hydrogen atoms were refined anisotropically using a full-matrix, least-squares technique. The hydrogen atoms were treated as 'riding' on their parent carbon atoms and assigned isotropic temperature factors of 1.2 (non-methyl) and 1.5 (methyl) times the value of equivalent temperature factor of the parent atom. The methyl groups were allowed to rotate about their local threefold axis. The SHELXS-97 and SHELXL-97 programs[20] were used for all the calculations.

Selected crystallographic data for $C_{17}H_{14}N_2O_2$ (L): monoclinic, space group $P2_1/c$, a = 13.7263(13), b = 11.3149(11) and c = 9.1935(9) Å, β = 103.803(9)°, V = 1386.6(2) $Å^3$, Z = 4, d_{calc} = 1.333 g cm^{-3}; μ = 0.089 mm^{-1}; data/restraints/parameters 2447/0/191; S = 0.998. Final R indices [$I > 2\sigma(I)$]: R_1 = 0.0446, wR_2 = 0.0966. R indices (all data): R = = 0.0731, wR = 0.1070.

Selected crystallographic data for $C_{34}H_{26}N_4O_4Pd$ ([$Pd(L)_2$]): triclinic, space group $P\bar{1}$, a = 4.8859(3), b = 9.0453(5) and c = 16.0294(11) Å, α = = 89.011(5), β = 87.620(6), γ = 83.387(5)°, V = 703.04(8) $Å^3$, Z = 1, d_{calc} = = 1.561 g cm^{-3}; μ = 0.708 mm^{-1}; data/restraints/parameters: 2480/0/232; S = 1.049. Final R indices [$I > 2\sigma(I)$]: R_1 = 0.0580, wR_2 = 0.1291. R indices (all data): R = 0.0620, wR = 0.1315.

CCDC 928019 and 936303 contain the supplementary crystallographic data for this paper. These data can be obtained free of charge from The Cambridge Crystallographic Data Centre *via* www.ccdc.cam.ac.uk. For details, see 'Notice to Authors', *Mendeleev Commun.*, Issue 1, 2014.

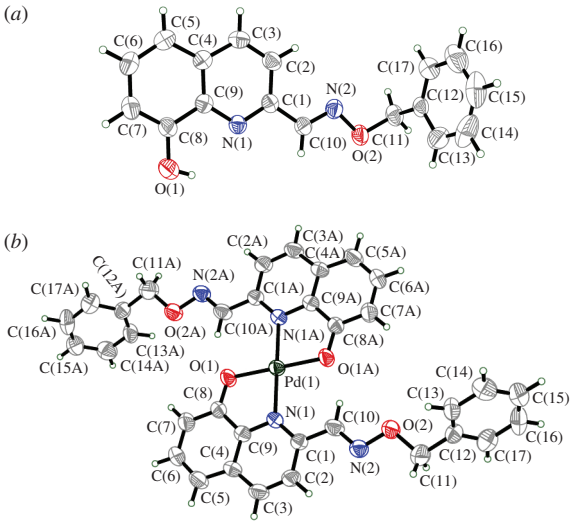

Figure 1 Molecular structures of (*a*) (*E*)-8-hydroxyquinoline-2-carbaldehyde *O*-benzyl oxime (L) and (*b*) [Pd(L)$_2$] complex with anisotropic displacement parameters shown at a 50% probability level.

characteristic bands of the C=C and C=N stretching modes appear at 1560 cm^{-1} in free ligand and are shifted to 1554 cm^{-1} in the complex. The shift is connected with C=C and C=N bonds elongation by about 0.02 Å upon coordination (see Table S2 in Online Supplementary Materials). The bond lengths in oxime part are slightly shorter in the complex than in free ligand, which is in accordance with IR spectra.

(*E*)-8-Hydroxyquinoline-2-carbaldehyde *O*-benzyl oxime (L) and its palladium(II) complex ([Pd(L)$_2$]) crystallize in monoclinic $P2_1/c$ and triclinic $P\bar{1}$ space group, respectively, and their molecular structures are presented in Figure 1. The structures are stabilized by short contacts, which can be classified as weak hydrogen bonds and π-stacking interactions (see Tables S3, S4 and Figure S1 in Online Supplementary Materials). The palladium(II) atom in complex [Pd(L)$_2$] has square planar environments with the ligands bonded to the metal through the pyridine nitrogen and hydroxyl oxygen atoms. Because the palladium atom in the complex structure is located on an inversion centre, the asymmetric unit contains one half of the complex. The Pd–N and Pd–O bond lengths of 2.076(4) and 1.986(3) Å, respectively, are comparable with those in other palladium(II) complexes. The square planar environment of palladium is distorted and the deviation from the expected 90° comes from the bite angle of ligand [O(1)–Pd(1)–N(1) 81.95(14)°].

The geometry of the complex was optimized in a singlet state by the DFT method with B3LYP functional using the Gaussian09 software package.[15,16] The B3LYP method in combination with DZVP basis[17] gives a good estimation of the Pd–N and Pd–O bond lengths (Table S2 in Online Supplementary Materials). The calculated charge on the palladium atom (0.77) is considerably lower than the formal +2. Moreover, the populations of the Pd(II) d_{xy}, d_{xz}, d_{yz}, $d_{x^2-y^2}$ and d_{z^2} orbitals of 1.74, 1.86, 2.00, 1.96 and 1.19, respectively, indicate a significant charge donation from the ligand. The NBO analysis shows meaningful advantage of donation from ligands to metal (563.6 kcal mol^{-1}) over Pd→L$_2$ backdonation (33.9 kcal mol^{-1}). The Pd–L interaction has a Coulomb-type character, which is visible in the calculated Wiberg bond indices with values considerably lower than one (Pd–N, 0.38; Pd–O, 0.47). The charge flow data indicate the strong σ-donor property of the ligand, which manifests itself in a significant population on b_{1g} level ($d_{x^2-y^2}$). The splitting of 4*d* palladium orbital diagram is presented in Online Supplementary Materials (Figure S2). The relatively large difference in energy between b_{2g} (π^*_{xy}) and b_{1g} ($\sigma^*_{x^2-y^2}$) levels (2.80 eV) also indicates the (*E*)-8-hydroxyquinoline-2-carbaldehyde *O*-benzyl oxime as a strong ligand.

The UV-VIS spectrum of the complex presents a broad unsymmetrical band with maxima at 347 and 333 nm and two maxima at 239 (sh.) and 212 nm. The electronic spectrum was calculated with the TD-DFT method and the solvent (acetonitrile) effect was simulated using the polarizable continuum model with the integral equation formalism (IEF-PCM).[18] The metal-to-ligand charge transfer transitions play a role at the lower energy bands with an admixture of LLCT transitions. In the higher energy part of spectrum, transitions from ligand to b_{1g} term ($\pi_L \rightarrow d_{x^2-y^2}$) were calculated. Generally, terms result from splitting, in D_{2h} ligand field, palladium 4*d* orbitals play a role in the whole spectrum, which is connected with the square planar geometry of the complex and a large nephelauxetic effect of the 4*d* orbitals. (The inset in Figure S2 presents density-of-states diagram for [Pd(L)$_2$] complex, and one can see that the palladium *d*-orbitals play role in a wide energy range of occupied molecular orbitals.)

Emission characteristics of the complex were obtained in optically diluted acetonitrile solutions at room temperature.¶ The solution of the complex was excited in a range of 250–500 nm, and fluorescence with a maximum at 398 nm by the excitation at 303 nm was observed (Figure 2). The red shift of the emission maximum is typical of 4*d* metal(II) complexes and the emission originating from the charge transfer states, derived from the excitations involving a $d_\pi \rightarrow \pi^*_L$ transitions. The quantum efficiency of 0.13 is rather high. In the solid state the emission has been quenched. The solution of the ligand does not exhibit emission upon excitation in a range from 200 to 350 nm.

Thus, (*E*)-8-hydroxyquinoline-2-carbaldehyde *O*-benzyl oxime and the palladium(II) complex with this ligand were synthesized; their molecular structures were determined by X-ray analysis, and the IR, NMR and UV-VIS spectra were studied. Based on the crystal structures, computational studies were carried out in order to determine the electronic structure of the complex. Electronic spectrum was calculated using the TD-DFT method and character of transitions was commented in connection with the structure of molecular orbitals. Excitation of an acetonitrile solution of the complex at 303 nm gave blue emission with a maximum at 398 nm (in the solid state, the emission is quenched).

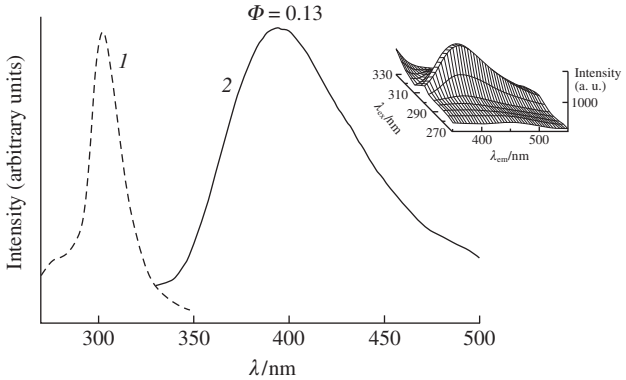

Figure 2 (*1*) Excitation and (*2*) fluorescence spectra of an acetonitrile solution of [Pd(L)$_2$]. Insert: the 3D fluorescence map.

¶ Quantum yields of fluorescence were calculated using the equation $\Phi_s = \Phi_{std}\mathrm{Grad}_s\eta_s^2/\mathrm{Grad}_{std}\eta_{std}^2$, where Φ_s is the quantum yield of unknown sample; Φ_{std} is the quantum yield of naphthalene as reference at 313 nm equal to 0.21; Grad_s and Grad_{std} are the gradients from the plot of integrated fluorescence intensity *vs.* the solutions absorbance at the excitation wavelength and η_s and η_{std} are the refractive indices of the solvents. Samples were prepared with absorbance less than 0.1 at excitation wavelengths in order to minimize re-absorption effects and avoid inner-filter effects, which may perturb the quantum yields. Solvent (acetonitrile) was of spectroscopic grade.

Emission originating from the lowest energy metal to ligand charge transfer (MLCT) state, derived from the excitation involving a $d_\pi \rightarrow \pi_L^*$ transition (with admixture of LLCT transitions) was observed. The assignment is supported by the analysis of the frontier orbitals of the complex showing a partial contribution of ligands nature.

The GAUSSIAN-09 calculations were carried out at the Wroclaw Centre for Networking and Supercomputing (WCSS) Poland, http://www.wcss.wroc.pl.

Online Supplementary Materials

Supplementary data associated with this article can be found in the online version at doi:10.1016/j.mencom.2013.12.008.

References

1 D. Kovala-Demertzi, M. A. Demertzis, E. Filiou, A. A. Pantazaki, P. N. Yadav, J. R. Miller, Y. Zheng and D. A. Kyriakidis, *Biometals*, 2013, **16**, 411.
2 E. Budizisz, U. Krajewska, M. Rozalski, A. Szulawska, M. Czyż and B. Nawrot, *Eur. J. Pharmacol*., 2004, **502**, 59.
3 J. Kuduk-Jaworska, A. Puszko, M. Kibiak and M. Pelczynska, *J. Inorg. Biochem.*, 2004, **98**, 1447.
4 E. Budzisz, M. Miernicka, I-P. Lorenz, P. Mayer, U. Krajewska and M. Rozalki, *Polyhedron*, 2009, **28**, 637.
5 Y. Najajreh, J. M. Perez, C. Navarro-Ranninger and D. Gibson, *J. Med. Chem*., 2002, **45**, 5189.
6 E. Khazanov, Y. Barenholtz, D. Gibson and Y. Najajreh, *J. Med. Chem.*, 2002, **45**, 5196.
7 N. Andrade-Lopez, J. G. Alvarado-Rodrıguez, S. Gonzalez-Montiel, M. G. Rodrıguez-Mendez, M. E. Paez-Hernandez and C. A. Galan-Vidal, *Polyhedron*, 2007, **26**, 4825.
8 S. O. Ojwach, I. A. Guzei, J. Darkwa and S. F. Mapolie, *Polyhedron*, 2007, **26**, 851.
9 L. Ma, R. C. Smith and J. D. Protasiewicz, *Inorg. Chim. Acta*, 2005, **358**, 3478.
10 E. Guney, V. T. Yilmaz and C. Kazak, *Polyhedron*, 2010, **29**, 1285.
11 V. Anbalagan and T. S. Srivastava, *Polyhedron*, 2004, **23**, 3173.
12 J. G. Małecki and P. Zwoliński, *Polyhedron*, 2012, **39**, 85.
13 J. G. Małecki and A. Maroń, *Transition Met. Chem*., 2011, **36**, 297.
14 J. G. Małecki, *J. Coord. Chem*., 2013, **66**, 1561.
15 A. D. Becke, *J. Chem. Phys*., 1993, **98**, 5648.
16 M. J. Frisch, G. W. Trucks, H. B. Schlegel, G. E. Scuseria, M. A. Robb, J. R. Cheeseman, G. Scalmani, V. Barone, B. Mennucci, G. A. Petersson, H. Nakatsuji, M. Caricato, X. Li, H. P. Hratchian, A. F. Izmaylov, J. Bloino, G. Zheng, J. L. Sonnenberg, M. Hada, M. Ehara, K. Toyota, R. Fukuda, J. Hasegawa, M. Ishida, T. Nakajima, Y. Honda, O. Kitao, H. Nakai, T. Vreven, J. A. Montgomery, Jr., J. E. Peralta, F. Ogliaro, M. Bearpark, J. J. Heyd, E. Brothers, K. N. Kudin, V. N. Staroverov, R. Kobayashi, J. Normand, K. Raghavachari, A. Rendell, J. C. Burant, S. S. Iyengar, J. Tomasi, M. Cossi, N. Rega, J. M. Millam, M. Klene, J. E. Knox, J. B. Cross, V. Bakken, C. Adamo, J. Jaramillo, R. Gomperts, R. E. Stratmann, O. Yazyev, A. J. Austin, R. Cammi, C. Pomelli, J. W. Ochterski, R. L. Martin, K. Morokuma, V. G. Zakrzewski, G. A. Voth, P. Salvador, J. J. Dannenberg, S. Dapprich, A. D. Daniels, O. Farkas, J. B. Foresman, J. V. Ortiz, J. Cioslowski and D. J. Fox, *Gaussian 09, Revision A.1*, Gaussian Inc., Wallingford CT, 2009.
17 N. Godbout, D. R. Salahub, J. Andzelm and E. Wimmer, *Can. J. Chem*., 1992, **70**, 560.
18 M. E. Casida, in *Recent Developments and Applications of Modern Density Functional Theory, Theoretical and Computational Chemistry*, ed. J. M. Seminario, Elsevier, Amsterdam, 1996, vol. 4, p. 391.
19 *CrysAlis RED*, Oxford Diffraction Ltd., Version 1.171.35.21, 2012.
20 G. M. Sheldrick, *Acta Crystallogr., Sect. A*, 2008, **64**, 112.

Received: 15th August 2013; Com. 13/4183